Electronic Supplementary Information (ESI)

Butylated melamine formaldehyde as a durable and highly positive friction layer for stable, high output triboelectric nanogenerators

Sung Soo Kwak, [a‡] SeongMin Kim,[a‡] Hanjun Ryu,[a] Jihye Kim,[a] Usman Khan,[a] Hong-Joon Yoon,[a] Yo Han Jeong,[b] and Sang-Woo Kim[*a,b]

[a]School of Advanced Materials Science and Engineering, Sungkyunkwan University (SKKU), Suwon, 16419, Republic of Korea

[b]SKKU Advanced Institute of Nanotechnology (SAINT), Sungkyunkwan University (SKKU), Suwon, 16419, Republic of Korea

*Correspondence to : kimsw1@skku.edu (S.-W. Kim)

‡S. S. Kwak and S.M. Kim contributed equally to this work

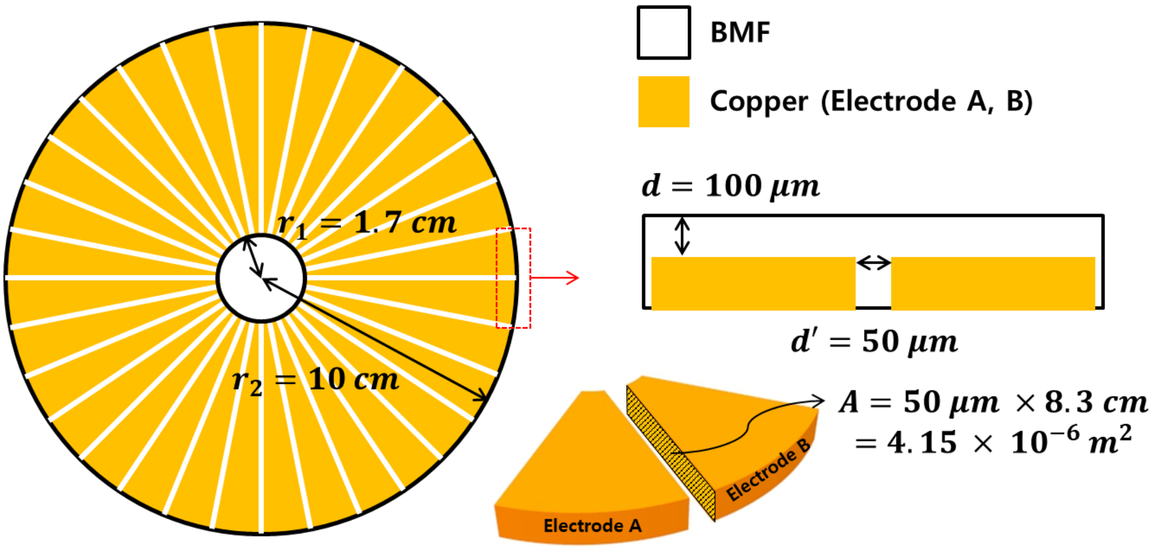

Supplementary Figure 1. A schematic model of metal-to-dielectric rotary freestanding TENG (RF-TENG). (top view)

Supplementary Table 1. Parameters used in the analytic calculation for metal-to-dielectric RF-TENG.

Dielectric constant ε_r	1.13 (Butylated melamine formaldehyde)
Dielectric thickness d	$100\ [\mu m]$
Inner radius r_1 of RF-TENG	$1.7\ [cm]$
Outer radius r_2 of RF-TENG	$10\ [cm]$
Grating number N	16 (Selected, for example)
Center angle of grating unit θ_0	$\frac{2\pi}{32} = \frac{\pi}{16}$ $(32\ segments)$
Angle velocity ω of rotation	$\left(\frac{300}{60}\right)2\pi = 10\pi\ [rad/s]$
Vacuum permittivity ε_0	$8.854 \times 10^{-12}\ [F/m]$
Parasitic capacitance C_P	$\varepsilon_0 \varepsilon_r \frac{A}{d'} = 4.98 \times 10^{-13}\ [F]$

Supplementary Note 1. RF-TENG master equations to derive the relationship between the current and the triboelectric charge density

Based on the ordinary differential equation of RF-TENG describing the load characteristics, some parameters including the boundary condition $Q(t=0)=Q_0$ and $Q(t=\frac{\theta_0}{\omega})=Q_1$ are defined and calculated first as shown below.

$$Q_0=\frac{N\sigma\theta_0({r_2}^2-{r_1}^2)-\left(-\frac{a}{b}\right)^{A_1}\int_0^{\frac{\theta_0}{\omega}}\frac{A_2t}{(a-t)(t-b)}\left(\frac{a-t}{t-b}\right)^{A_1}dt}{\left(-\frac{a}{b}\right)^{2A_1}+1}=0.012\sigma \quad \text{................ (S1)}$$

$$Q_1=Q\left(\frac{\theta_0}{\omega}\right)=\left(\frac{a}{-b}\right)^{A_1}\int_0^{\frac{\theta_0}{\omega}}\frac{A_2t}{(a-t)(t-b)}\left(\frac{a-t}{t-b}\right)^{A_1}dt+\left(\frac{a}{-b}\right)^{2A_1}Q_0=0.019\sigma \quad \text{................ (S2)}$$

$$a=\frac{\theta_0}{2\omega}+\frac{1}{2}\sqrt{\frac{{\theta_0}^2}{\omega^2}+\frac{8d\theta_0C_p}{N\varepsilon_0\varepsilon_r\omega^2({r_2}^2-{r_1}^2)}}=0.006252\ [s] \quad \text{................ (S3)}$$

$$b=\frac{\theta_0}{2\omega}-\frac{1}{2}\sqrt{\frac{{\theta_0}^2}{\omega^2}+\frac{8d\theta_0C_p}{N\varepsilon_0\varepsilon_r\omega^2({r_2}^2-{r_1}^2)}}=-2.03\times10^{-6}\ [s] \quad \text{................ (S4)}$$

$$A_1=-\frac{2d\theta_0}{NR\varepsilon_0\varepsilon_r\omega^2({r_2}^2-{r_1}^2)\sqrt{\frac{{\theta_0}^2}{\omega^2}+\frac{8d\theta_0C_p}{N\varepsilon_0\varepsilon_r\omega^2({r_2}^2-{r_1}^2)}}}=-0.10231 \quad \text{................ (S5)}$$

$$A_2=\frac{2d\theta_0\sigma}{R\varepsilon_0\varepsilon_r\omega}=0.0031\sigma\ [C]=0.0031\left(\frac{Q_{tribo}}{A}\right)[C] \quad \text{................ (S6)}$$

The right part of each equation is obtained by substituting the parameter value in Table S1 into the equation.

After getting the charge Q_1 from which the current I was calculated by differentiating Q for the first and second half cycle respectively as shown below.

$$I=\frac{A_1(a-b)}{(a-t)(t-b)}\left(\frac{a-t}{t-b}\right)^{-A_1}\left[\int_0^t\frac{A_2t}{(a-t)(t-b)}\left(\frac{a-t}{t-b}\right)^{A_1}dt+\left(\frac{a}{-b}\right)^{A_1}Q_0\right]$$

$$+\frac{A_2t}{(a-t)(t-b)},\left(0\le t\le\frac{\theta_0}{\omega}\right)\ :\ 1^{\text{st}}\text{ half cycle} \quad \text{................ (S7)}$$

$$I(t)=\sigma\left(6.3\times10^{-9}+1.6\times10^{-5}\left(\frac{6.2\times10^{-3}-1.t}{2.0\times10^{-6}+t}\right)^{0.1}-\frac{3.1\times10^{-3}t}{(-6.2\times10^{-3}+t)(2.0\times10^{-6}+t)}+(-6.3\times10^{-9}-(3.1\times\right.$$

$$\left.`10^{-3})t)\ Hypergeometric2F1\ [1,\ 1,\ 8.9\times10^{-1},\ 9.9\times10^{-1}-(1.5\times10^2)t]\right)=\sigma\times f(t) \quad \text{................ (S8)}$$

$$I=\frac{A_1(a-b)}{\left(a-t+\frac{\theta_0}{\omega}\right)\left(t-\frac{\theta_0}{\omega}-b\right)}\left(\frac{a-t+\frac{\theta_0}{\omega}}{t-\frac{\theta_0}{\omega}-b}\right)^{-A_1}\left\{[Q_1-N\sigma\theta_0({r_2}^2-{r_1}^2)]\left(\frac{a}{-b}\right)^{A_1}-\int_0^t\frac{A_2t}{(a-t)(t-b)}\left(\frac{a-t}{t-b}\right)^{A_1}dt\right\}$$

$$-\frac{A_2\left(t-\frac{\theta_0}{\omega}\right)}{\left(a-t+\frac{\theta_0}{\omega}\right)\left(t-\frac{\theta_0}{\omega}-b\right)},\left(\frac{\theta_0}{\omega}\le t\le\frac{2\theta_0}{\omega}\right)\ :\ 2^{\text{nd}}\text{ half cycle} \quad \text{................ (S9)}$$

$$I(t) = \frac{3.1\times10^{-3}(-6.2\times10^{-3}+t)\sigma}{(-1.2\times10^{-2}+t)(-6.2\times10^{-3}+t)} - (1.6\times10^{-5})\sigma\left((3.8\times10^{-4}+1.\ \left(\frac{1.2\times10^{-2}-1.t}{-6.2\times10^{-3}+1.t}\right)^{0.1} + (1.1-(1.8\times10^{2})t)\ Hypergeometric2F1[1,\ 1,\ 8.9\times10^{-1},\ 1.9-(1.5\times10^{2})t]\right) = \sigma\times f'(t) \qquad \cdots\cdots\cdots\ \text{(S10)}$$

As explained in the above statement, the determining factors that influence the current pattern I are triboelectric charge density, σ and some general function, $f(t)$ where I is directly proportional to σ $(=\frac{Q_{tribo}}{A})$.

Supplementary Note 2. Calculation of the equivalent galvanostatic current

The equivalent galvanostatic current I_{eg} is calculated by following equation,

$$I_{eg} = \frac{C \times \Delta V}{\Delta t} \qquad \text{................ (S11)}$$

Where C is capacitance of the capacitor integrated, ΔV is the voltage change during the charging or discharging time Δt. According to the Fig. 4e experimental result, the C is 4.8 μF, ΔV is 13 V (from 5 V to 18 V), Δt is about 0.325 sec (from 0.992 sec to 1.325 sec). Therefore, I_{eg} is over 191.75 μA.

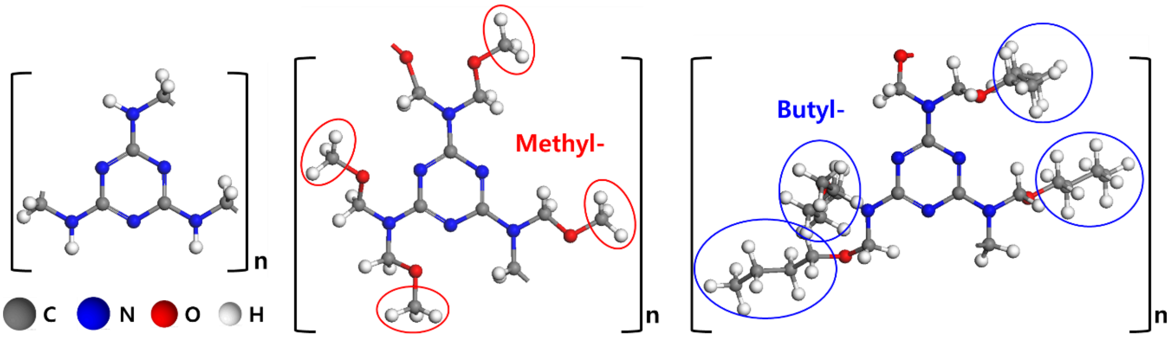

Supplementary Figure 2. Schematic description of the chemical structure of the three MFs: pristine, methylated and butylated.

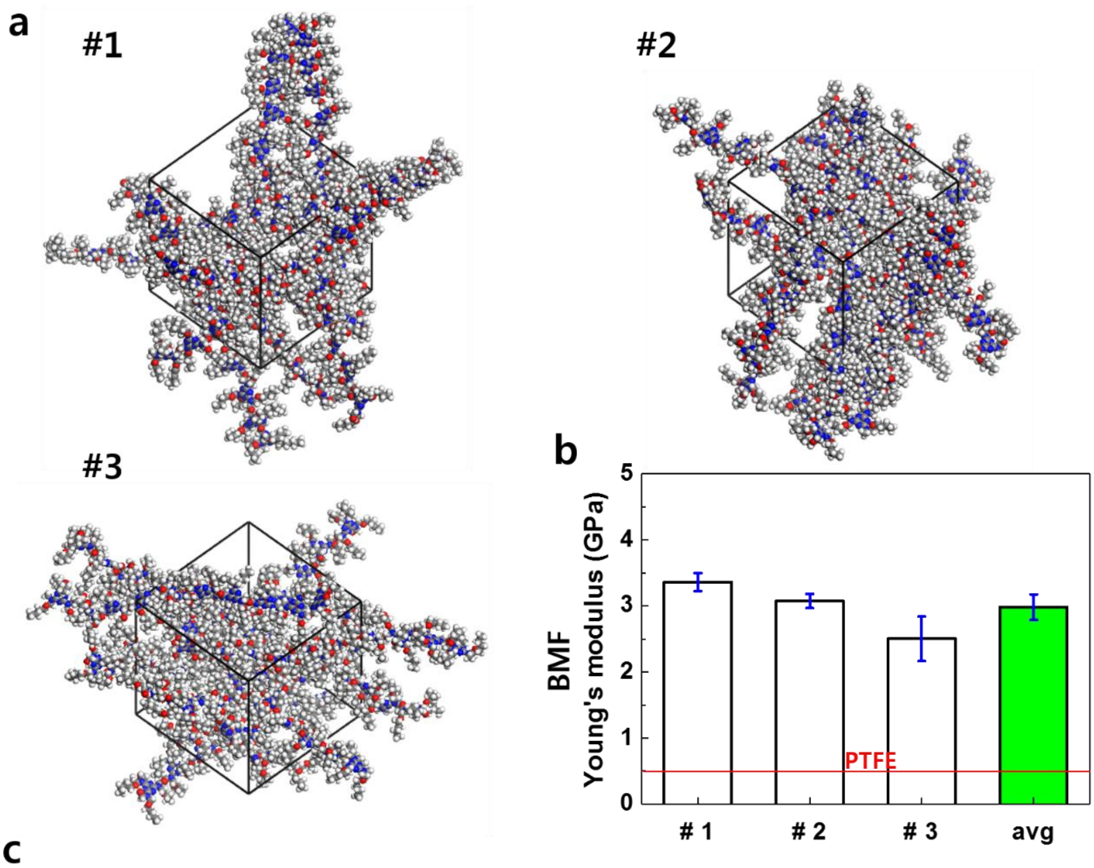

c

Sample	Young's modulus [*GPa*]				
	X	*Y*	*Z*	*Average*	*Standard-deviation*
BMF #1	**3.521**	**3.046**	**3.516**	**3.361**	**0.273**
BMF #2	**3.317**	**2.904**	**2.998**	**3.073**	**0.216**
BMF #3	**2.849**	**2.940**	**1.727**	**2.505**	**0.676**

Supplementary Figure 3. Results of MD simulation for BMF. (a) Three different BMF amorphous cells with stable structure obtained through the geometric optimization. (b) Comparison of the calculated Young's modulus values of BMFs in each structure with the Young's modulus of PTFE. (c) For the three BMF amorphous cells, the Young's moduli in the three axial directions, and their average and standard deviation.

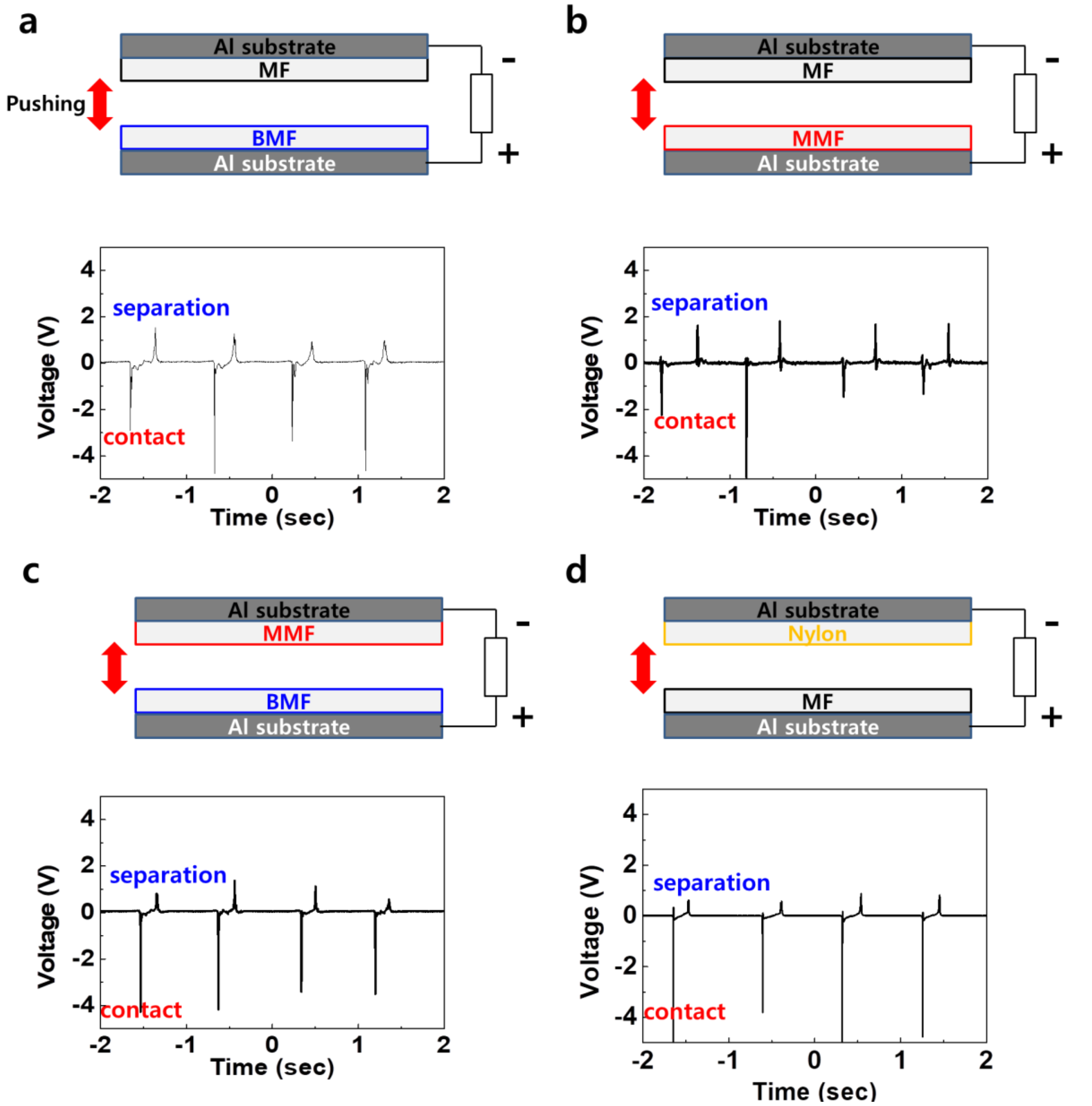

Supplementary Figure 4. Triboelectric characterization of the three MFs using contact-separation and comparison with nylon. Triboelectric output voltage with (a) MF/BMF, (b) MF/MMF, (c) MMF/BMF and (d) MF/Nylon as the friction pair; peak direction shows that BMF is the most positive among the three MFs.

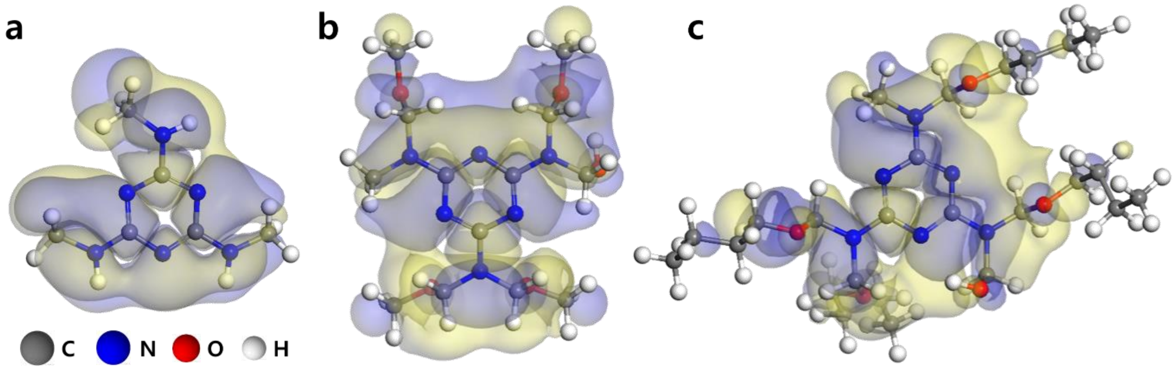

Supplementary Figure 5. LUMO distribution of the three MFs calculated by DFT simulation: (a) pristine MF, (b) MMF, and (c) BMF.

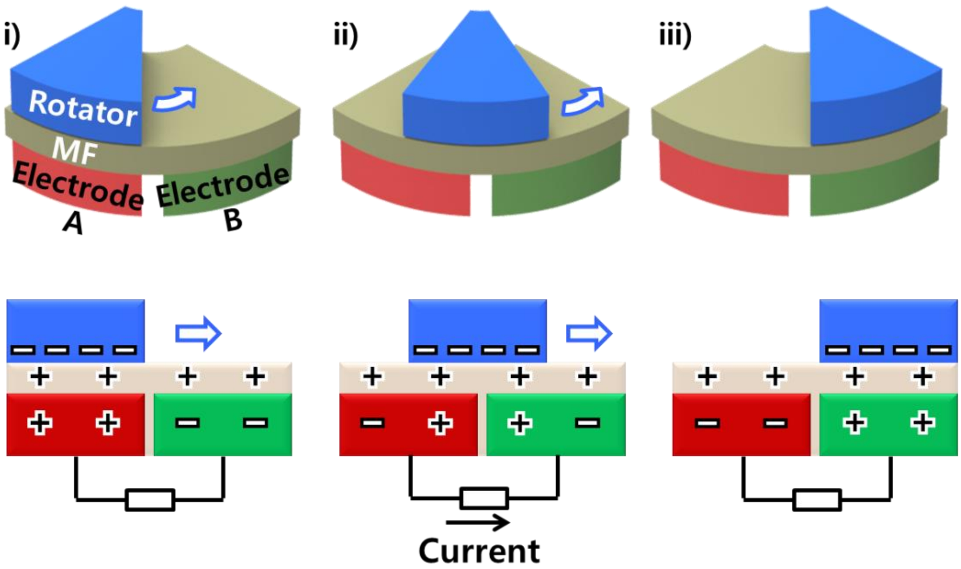

Supplementary Figure 6. Schematic description of working mechanism of the electricity generation using the MF TENG when rotating. The working mechanism is based on a coupling effect between the triboelectrification and electrostatic induction. Rotation leads to the triboelectrification between the MF of the stator and the Cu of the rotator and, as a consequence, the MF and Cu have positive and negative charges, respectively, on their surfaces. After full contact by rotation, the same amount of triboelectric charges are formed on each surface, but since the area of Cu is half that of MF, the density of negative charge on Cu (σ_{Cu}) is twice the density of positive charge on MF (σ_{MF}). Initially, a Cu sector on the rotator is facing the electrode A, and the charges on the MF surface and the A electrodes fully screen the charges on the rotating Cu sector. As the rotator rotates by half of the central angle of a Cu sector, such that the rotating Cu sector is oriented between the A and B Cu electrodes, there is a charge transfer/redistribution between the A and B electrodes, in order to screen the charges on the rotating Cu sector, thereby generating a current flow from electrodes A and B. As the rotator rotates by a full central angle, the rotating Cu sector fully overlaps the electrode B, the charge transfer between electrodes A and B continues and is fully completed, which completes one half of the current cycle. On the other hand, when the rotator moves from electrode B to A, the charge transfer between electrodes A and B is in the opposite direction, thereby completing the opposite half of the current cycle. The periodically changing electric field under rotating motion, therefore, generates an alternating current flow through an external circuit, connected between electrodes A and B.

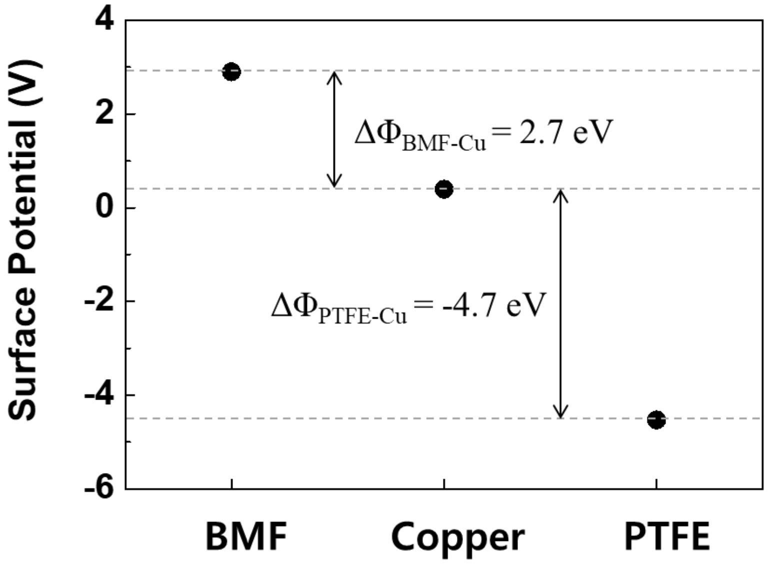

Supplementary Figure 7. Surface potential, measured using KPFM, of BMF, Cu and PTFE and the calculated work function difference of BMF and PTFE from Cu.

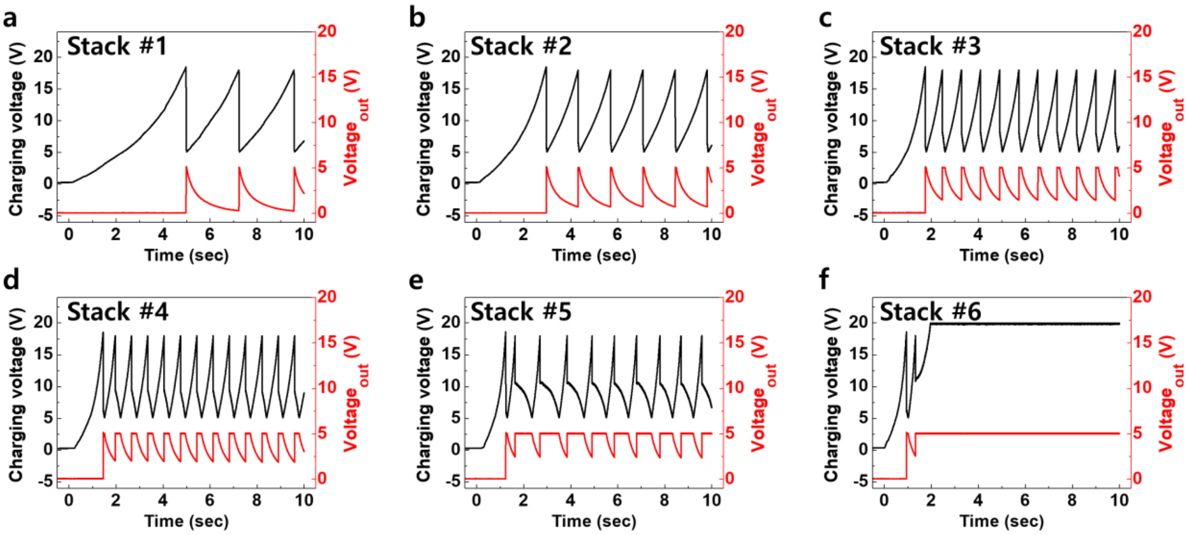

Supplementary Figure 8. Charging voltage of supercapacitor and voltage output from the PMIC when supplied by stacked BMF based TENGs; stacking of one to six TENGs.